

## MODELING OF ONE DIMENSIONAL ABLATION

Ratna Kumar.A.S, [sam\\_munna84@yahoo.com](mailto:sam_munna84@yahoo.com)  
Jefferson Raja Bose.B, [jefferson@karunya.edu](mailto:jefferson@karunya.edu)

Karunya University  
Karunya Nagar  
Coimbatore  
TamilNadu  
India-641114.

**Abstract.** *The development of a one-dimensional (planar) material thermal response with ablation is presented. The mixture energy equation, under uniform heat conduction is solved with Fourier's law to model heat conduction, and the ideal gas law to model the state of the pyrolysis gases. Consequently, the temperature, profile is predicted for a decomposing ablator. The control volume finite element spatial discretization method (CVFEM), the Euler implicit time integrator, and a contracting grid scheme are used for the solution of the mixture energy equation. The mixture energy equation is solved using segregated Newton solvers, which allow for nonlinear iteration on the entire system of nodal equations that are discretized according to a residual formulation. The block Gauss-Seidel segregated solution procedure has been implemented to globally iterate on the system of governing equations resulting in a fully coupled solution.*

**Keywords:** *Thermal Response, Ablation, control volume.*

### Nomenclature

A	Area
$\mathbf{A}$	Area vector
h	Specific enthalpy
$\bar{E}$	Energy content
$\dot{m}''$	Mass flux
$\dot{m}'''$	Volumetric mass source term
$q''$	Heat flux
$\mathbf{q}''$	Heat flux vector

$\hat{M}$	Molecular weight
$s$	Surface recession
$\dot{s}$	Surface recession rate
(e)	Element
T	Temperature
t	Time
z	Coordinate with respect to initial ablation front
$\dot{z}$	Nodal velocity

### Greek symbols

$\Gamma$	Initial resin volume fraction
$\eta$	Landau coordinate
$\xi$	Local coordinate
$\psi$	Reaction order in Arrhenius relationship
$\rho$	Density

### Subscripts

i	Composite component index
c	Char
cv	Control volume
s	Solid
v	Virgin plastic
g	Gas

### Superscripts

n	Time level
v	Iteration level

## 1. Introduction

Ablation has been defined as self regulating heat and mass transfer process in which incident thermal energy is expended by sacrificial loss of material.

Charring ablators provide the most efficient TPS for aerospace applications. These are being processed by the method of synthetic assembly of resin binder and a refractory reinforcement in order to obtain certain special characteristics and properties. The char is a thermal insulation, the interior of which is cooled by volatile material percolating through it from decomposing polymer (Figure.1). A thick char provides an efficient insulation barrier, reradiates a large amount of incoming heat from the surface, and is a very efficient ablator. Very good char strength has been obtained with carbon phenolic TPS materials.

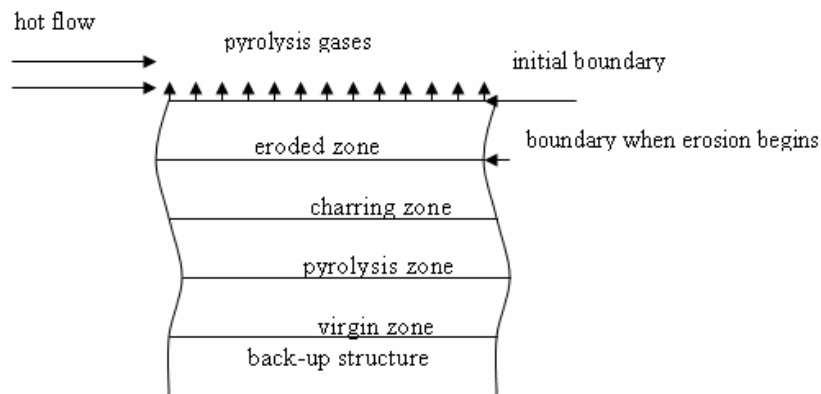


Figure 1. Heat transfer mechanism of charring ablators under hot flow

### 1.1 Literature Review

Aerotherm Corporation, one of NASA's contractors developed Charring Materials Ablation (CMA), and it has served as the industry standard for several decades. CMA is a one-dimensional material thermal response code with in-depth decomposition that solves the energy equation with pyrolysis gas effects. One of the primary physical assumptions that the developers, Moyer and Rindal [9], made was that for a given time step, the pyrolysis gas generated further in-depth than a given node was assumed to flow past that node during the time step. In terms of numerics, CMA has a finite difference spatial discretization of the governing differential equations and the Euler implicit time integrator. Moyer and Rindal implemented a translating grid scheme in which the grid is attached to the receding surface and the overall number of nodes in the domain is reduced as mass is removed at the ablating surface. Since the energy equation is nonlinear in both surface recession rate and temperature, a linearization method is necessary to find a solution. Moyer and Rindal accomplished this by lagging the thermo-physical properties and surface recession rate one time step for the interior node equations while they iteratively solve the surface energy balance to find the updated recession rate.

Recently J.L.Lin, C.S.Yang [5] presented experimental and numerical work under the aerodynamic heating of charring ablators. The experiment model is a stainless steel cone with an attached charring ablator, in which supersonic hot flow impinges and the numerical simulation is based on physical and mathematical models including one dimensional unsteady energy transport and mass conservation equations coupled with calculations of aerodynamic heating, thermal degradation, heat transfer of the ablating surface and the ablation model. The findings from the numerical calculations are time history of temperature distribution inside the charring material and the backup structure

### 1.2 Present work

The study is focused to obtain the temperature profile for the effective design of the back-up structure under the assumption of steady state conduction, in finite volume method considering the effect variations in material and thermo-physical properties.

### 2. Mathematical modeling

Under the assumptions that the pyrolysis gas is a single non-reactive entity, the solid and gas are in thermal equilibrium, and there is no in-depth energy source, then the solid and gas energy equations for a moving grid reduce to a mixture energy equation given by

$$\int_{cs} \dot{q} \cdot dA + \int_{cs} \phi \rho_g h_g v_g \cdot dA - \int_{cs} \rho h v_{cs} \cdot dA + \frac{d}{dt} \int_{cv} \rho e dV = 0 \dots \dots (1)$$

#### 2.1. Boundary conditions

Arrays of boundary conditions for the mixture energy equation are studied and the most commonly used for engineering applications are convective aerodynamic heating and radiation. Assuming equal species diffusion coefficients and equal mass and heat transfer Stanton numbers, the aerodynamic heating/radiation boundary condition with ablative and pyrolysis gas flux energy terms is given by

$$\dot{q}'' = \rho_e u_e C_{ho} \left( \frac{C_h}{C_{ho}} \right) (h_w - h_r) + \varepsilon \sigma (T_{bnd}^4 - T_{res}^4) + \dot{m}_s'' h_w + \dot{m}_g'' h_w \dots \dots (2)$$

where  $C_h/C_{ho}$  is an empirical Stanton number correction for mass blowing and hot wall effects. The wall gas enthalpy ( $h_w$ ) is defined as the enthalpy resulting from equilibrated reactions between ablation products, pyrolysis gases being injected into the boundary layer, and boundary layer gases from the surrounding environment.

#### 2.2 Material Model

In order to complete the explanation of the governing equations and boundary conditions, it is important to understand the material model used to characterize the state of the solid/gas mixture. It is assumed that all the pores are interconnected, and therefore pyrolysis gases occupy all of the

pore space and are free to flow through it. Consequently, the density of the solid/gas mixture is described by

$$\rho = \phi \rho_g + \rho_s \dots (3)$$

In terms of units Eq.3 can be expressed as

$$\left[ \frac{\text{mixture mass}}{\text{mixture vol}} \right] = \left[ \frac{\text{pore vol}}{\text{mixture vol}} \right] \left[ \frac{\text{gas mass}}{\text{pore vol}} \right] + \left[ \frac{\text{solid mass}}{\text{mixture vol}} \right] \dots (4)$$

It is assumed that the thermodynamic state of the pyrolysis gases can be described by the perfect gas law, and that the solid and gas phases are in thermal equilibrium resulting in

$$P = \rho_g \frac{\hat{R}}{M_g} T_g \dots (5)$$

where

$$T_g = T_s = T$$

The solid material model adopted in this study is similar to [9, 13] solid bulk density is given by

$$\rho_s = \Gamma(\rho_A + \rho_B) + (1 - \Gamma)\rho_C \dots (6)$$

The reaction is irreversible, and the pyrolysis gases are assumed to not react among them or with the remaining solid in the pore space. Taking the temporal derivative of Eq. (6) gives the solid decomposition rate in terms of component decomposition rates.

$$\frac{\partial \rho_s}{\partial t} = \Gamma \left( \frac{\partial \rho_A}{\partial t} + \frac{\partial \rho_B}{\partial t} \right) + (1 - \Gamma) \frac{\partial \rho_C}{\partial t} \dots (7)$$

It is assumed that the decomposition of each component can be described by an Arrhenius relationship of the form

$$\frac{\partial \rho_i}{\partial t} = -K_i \rho_{v_i} \left( \frac{\rho_i - \rho_{c_i}}{\rho_{v_i}} \right)^{\psi_i} e^{-E/RT} \text{ for } i = A, B \text{ and } c \dots (8)$$

which applies at a constant spatial location.

The intermediate solid is modeled as some interpolated state between virgin and char. This interpolated state is characterized by the extent of reaction ( $\beta$ ), or degree of char, given by

$$\beta = \frac{\rho_v - \rho_s}{\rho_v - \rho_c} \dots (9)$$

In a similar light CMA [9] defines imaginary virgin mass fraction

$$y_v = \frac{\rho_v}{\rho_v - \rho_c} \left( 1 - \frac{\rho_c}{\rho_s} \right)$$

### 2.3. Property Model

Discussions of properties are required for the solution of governing equation therefore thermo-physical and thermodynamic properties which are input parameters are given in the following table.

**Table 1: Thermo-physical and thermodynamic property input parameters**

Input parameter	Description
$C_{v_v}(T)$	Specific heat of virgin material Vs. Temp
$C_{v_c}(T)$	Specific heat of char material Vs. Temp
$T_{ref}$	Reference temp. for heat of formation
$(h_f^o)_v$	Virgin plastic heat of formation
$(h_f^o)_c$	Char heat of formation
$(h_f^o)_g$	Pyrolysis gas heat of formation
$k_v(T)$	Thermal conductivity of the virgin material Vs. Temp
$k_c(T)$	Thermal conductivity of the char material Vs. Temp
$\epsilon_c(T)$	Emissivity of virgin material Vs. Temp
$\epsilon_v(T)$	Emissivity of char material Vs. Temp
$h_g(T)$	Pyrolysis gas enthalpy Vs. Temp
$\bar{M}_g(T)$	Pyrolysis gas molecular weight Vs. Temp
$\phi(\beta)$	Porosity Vs. Extent of reaction
$\kappa(\beta)$	Permeability Vs. Extent of reaction
$\mu(T)$	Pyrolysis gas dynamic viscosity Vs. Extent of reaction

### 2.4 Specific Internal Energy and Gas Enthalpy Models

The specific internal energy of the mixture will take into account both the solid and gas phases. The solid specific internal energy and enthalpy can be found from

$$e_s(T) = h_s(T) = y_v e_v(T) + (1 - y_v) e_c(T) \dots \dots \dots (10)$$

where  $e_v(T)$  and  $e_c(T)$  are determined by parabolic interpolation in the virgin and char specific internal energy tables and also provide details regarding parabolic interpolation routine.

### 2.4.1 Specific Internal Energy and Gas Enthalpy Table Generation

Through integration of the tabulated specific heat functions, specific internal energy tables can be generated for the virgin and char. The code requires an input reference temperature,  $T_{ref}$ , that will serve as the "zero" datum for both the specific internal energy functions and the pyrolysis gas specific enthalpy table. It is important to note that although the pyrolysis gas specific enthalpy is a function of pressure and temperature, it is assumed that there is weak pressure dependence, and therefore the gas enthalpy is a function of temperature only.

$$h_g(T) = [h_g(T)]_{i/p} + (h_f^0)_g \dots \dots (11)$$

so that the enthalpy at the reference temperature is consistent with the solid internal energy tables.

$$e(T_k) = h_f^0 - \int_{T_i}^{T_{ref}} C_v(T) dT \text{ for } k=1$$

$$= e(T_1) + \left[ \sum_{j=1}^{i-1} \frac{1}{2} [C_v(T_j) + C_v(T_{j-1})] (T_j - T_{j-1}) \right] \text{ for } k=2 \dots n \dots \dots (12)$$

### 2.5. Domain Description and Discretization Method

Before discussing the discretization of the governing equations and their respective solution procedures, it is necessary to provide a description of the coordinate systems, grid motion scheme, and spatial discretization method. The method uses the following grid generation:

1. Automatic non-uniform grid generation with a geometric progression based on domain length, number of elements specified, and either first or last element thickness where

$$\frac{\Delta z_{j+1}}{\Delta z_j}$$

and

$$\Delta z_j = z_{j+1} - z_j$$

#### 2.5.1 Spatial Discretization and Coordinate System

The control volume finite element method, which has been previously used for ablation problems [1, 15], associates a control volume with each node in the discretized domain. The method uses the co-ordinate system used in [15] to describe the surface recession with grid velocity.

### 3. Mixture Energy Equation

The mixture energy conservation equation

$$\int_{cs} \dot{q} \cdot dA + \int_{cs} \phi \rho_g h_g v_g \cdot dA - \int_{cs} \rho h v_{cs} \cdot dA + \frac{d}{dt} \int_{cv} \rho e dV = 0$$

where the discretization of each term is discussed in the subsequent sections. For both the mixture energy and gas mass conservation equations, a consistent sign convention is adopted such that

[Outflow terms] - [inflow terms] + [rate of change of content] = [source terms]

Therefore energy equation becomes

$$0 = \left( \dot{q} A \right)_{j+1/2} - \left( \dot{q} A \right)_{j-1/2} - \left( \phi \rho_g h_g u_{cs} A \right)_{j-1/2} + \left( \phi \rho_g h_g u_{cs} A \right)_{j+1/2} + \left( \rho h u_{cs} A \right)_{j-1/2} - \left( \rho h u_{cs} A \right)_{j+1/2} + \frac{d}{dt} \int_{z_{j-1}}^{z_j} \rho e dZ + \frac{d}{dt} \int_{z_j}^{z_{j+1}} \rho e dZ \dots \dots \dots (13)$$

and the energy balance terms can be seen in figure.2 Section 2.3 presented the model for determining thermo-physical and thermodynamic properties of the gas, solid, and mixture that are necessary for the solution of the mixture energy equation.

While solving the mixture energy equation, nodal temperatures and the surface recession rate are treated as the dependent variables while nodal values of solid density, gas density, and gas velocity are constant.

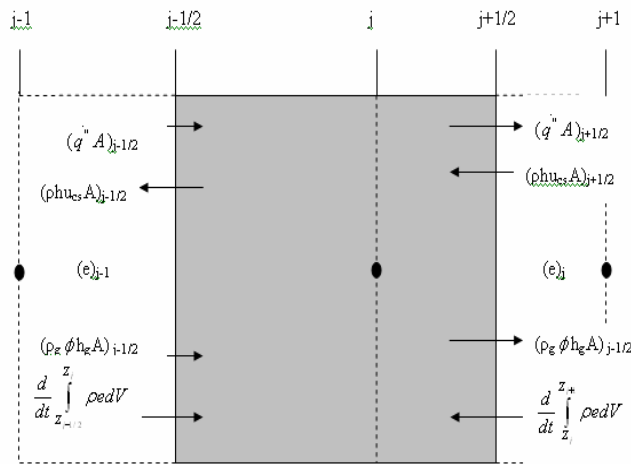


**Figure 2: Energy balance terms for the control volume surrounding node j**

The linear system, for the five node domain, is of the form in which there is non linear dependence on surface recession rate

$$\begin{pmatrix} e_0 & c_0 & 0 & 0 & 0 & 0 \\ e_1 & b_1 & c_1 & 0 & 0 & 0 \\ e_2 & a_2 & b_2 & c_2 & 0 & 0 \\ e_3 & 0 & a_3 & b_3 & c_3 & 0 \\ e_4 & 0 & 0 & a_4 & b_4 & c_4 \\ e_5 & 0 & 0 & 0 & a_5 & b_5 \end{pmatrix} \begin{pmatrix} \Delta s \\ \Delta T_1 \\ \Delta T_2 \\ \Delta T_3 \\ \Delta T_4 \\ \Delta T_5 \end{pmatrix} = \begin{pmatrix} d_0 \\ d_1 \\ d_2 \\ d_3 \\ d_4 \\ d_5 \end{pmatrix} \dots \dots \dots (14)$$

### 3.1. Conduction

Fourier's law is used to model the heat conducted at a control volume boundary and the heat conduction rate is given by

$$\dot{Q}_{j+1/2} = \left[ -k(T)A \frac{dT}{dz} \right]_{j+1/2} = \frac{-\bar{K}(T)A}{\Delta z_j} (T_{j+1} - T_j) \dots \dots \dots (15)$$

where  $\bar{X} = \frac{(X_{j+1} + X_j)}{2}$  and X is any quantity. The element representation of heat conduction is

$$\begin{bmatrix} \dot{Q}_j \\ \dot{Q}_{j+1} \end{bmatrix} = \frac{-\bar{K}(T)A}{\Delta z_j} \begin{bmatrix} 1 & -1 \\ -1 & 1 \end{bmatrix} \begin{bmatrix} T_j \\ T_{j+1} \end{bmatrix} \dots \dots \dots (16)$$

In general, the heat conduction vector is a nonlinear function of temperature and recession rate since the thermal conductivity depends on temperature and  $\Delta z_j$  depends on the surface recession rate. Therefore an iterative solution procedure is necessary to solve for the time accurate nonlinearities. To aid in the iterative process, it is convenient to linearize the element conduction vector with a Taylor series expansion in iteration space treating the nodal temperatures and surface recession rate as the independent variables

$$\begin{bmatrix} \dot{Q}_j \\ \dot{Q}_{j+1} \end{bmatrix}^{v+1} = \begin{bmatrix} \dot{Q}_j \\ \dot{Q}_{j+1} \end{bmatrix}^v + \begin{bmatrix} \frac{\partial \dot{Q}_j}{\partial s} & \frac{\partial \dot{Q}_j}{\partial T_j} & \frac{\partial \dot{Q}_j}{\partial T_{j+1}} \\ \frac{\partial \dot{Q}_{j+1}}{\partial s} & \frac{\partial \dot{Q}_{j+1}}{\partial T_j} & \frac{\partial \dot{Q}_{j+1}}{\partial T_{j+1}} \end{bmatrix} \begin{bmatrix} \Delta s \\ \Delta T_j \\ \Delta T_{j+1} \end{bmatrix}^{v+1} + \dots \dots \dots (17)$$

Performing the required differentiation for planar geometry ( $A(z) = 1$ ) gives

$$\left. \begin{aligned} \frac{\partial \dot{Q}_j}{\partial s} &= \frac{\bar{k}A}{\Delta z_j^2} (T_j - T_{j+1}) \frac{\partial \Delta z_j}{\partial s} \\ \frac{\partial \dot{Q}_{j+1}}{\partial s} &= \frac{\bar{k}A}{\Delta z_j^2} (T_j - T_{j+1}) \frac{\partial \Delta z_j}{\partial s} \\ \frac{\partial \dot{Q}_j}{\partial T_j} &= \frac{\bar{k}A}{\Delta z_j^2} \left[ 1 + \frac{(T_j - T_{j+1})}{2k} \left( \frac{\partial k}{\partial T} \right)_j \right] \\ \frac{\partial \dot{Q}_j}{\partial T_{j+1}} &= \frac{\bar{k}A}{\Delta z_j^2} \left[ -1 + \frac{(T_j - T_{j+1})}{2k} \left( \frac{\partial k}{\partial T} \right)_{j+1} \right] \\ \frac{\partial \dot{Q}_{j+1}}{\partial T_j} &= \frac{\bar{k}A}{\Delta z_j^2} \left[ -1 - \frac{(T_j - T_{j+1})}{2k} \left( \frac{\partial k}{\partial T} \right)_j \right] \\ \frac{\partial \dot{Q}_{j+1}}{\partial T_{j+1}} &= \frac{\bar{k}A}{\Delta z_j^2} \left[ 1 - \frac{(T_j - T_{j+1})}{2k} \left( \frac{\partial k}{\partial T} \right)_{j+1} \right] \end{aligned} \right\} \dots (18)$$

where

$$\frac{\partial \Delta z_j}{\partial s} = \Delta t^{n+1} (\eta_{j+1} - \eta_j) = \Delta t^{n+1} \Delta \eta_j \dots \dots (19)$$

### 3.2 Energy Content and Time Integration

The energy content for an element can be divided into terms corresponding to each of the two sub-control volumes within an element.

$$\begin{bmatrix} E_j \\ E_{j+1} \end{bmatrix} = \begin{bmatrix} \int_{z_j}^{\bar{z}_j} \rho e(T) A dz \\ \int_{z_j}^{z_{j+1}} \rho e(T) A dz \end{bmatrix} \dots \dots (20)$$

The internal energy per unit volume in Eq. (20) can be expressed by a Taylor series expansion in position about the element center

$$(\rho e)_z = (\rho e)_{\bar{z}_j} + \frac{\partial(\rho e)}{\partial z} \Big|_{\bar{z}_j} (z - \bar{z}_j) + \dots \dots \dots (21)$$

The elemental energy content vector can now be expressed as

$$\begin{bmatrix} E_j \\ E_{j+1} \end{bmatrix} = \begin{bmatrix} \int_{z_j}^{\bar{z}_j} \left( \overline{\rho e} + \frac{\partial(\rho e)}{\partial z} \Big|_{z=\bar{z}_j} (z - \bar{z}_j) \right) A dz \\ \int_{z_j}^{z_{j+1}} \left( \overline{\rho e} + \frac{\partial(\rho e)}{\partial z} \Big|_{z=\bar{z}_j} (z - \bar{z}_j) \right) A dz \end{bmatrix} \dots \dots (22)$$

where

$$(\rho e)_{\bar{z}_j} = \overline{\rho e} = \frac{1}{2} [(\rho e)_j + (\rho e)_{j+1}]$$

To aid in the integration process it is convenient to employ a local coordinate system in which the shape functions within an element are written as

$$\left. \begin{aligned} N_1(\xi) &= \frac{1}{2}(1 - \xi) \\ N_2(\xi) &= \frac{1}{2}(1 + \xi) = 1 - N_1(\xi) \end{aligned} \right\} \text{for } -1 < \xi < 1 \dots \dots (23)$$

the global coordinate  $z$ , and the local coordinate  $\xi$ , are related through

$$z = N_1(\xi) z_j + N_2(\xi) z_{j+1} = \bar{z}_j + \frac{\xi}{2} \Delta z_j \dots \dots (24)$$

and consequently the differential length is

$$dz = \frac{\Delta z_j}{2} d\xi$$

If a finite central difference is used to approximate  $\left(\frac{\partial(\rho e)}{\partial z}\right)$ , the energy

capacitance terms can be rewritten in terms of local coordinates as

$$\begin{bmatrix} \bar{E}_j \\ \bar{E}_{j+1} \end{bmatrix} = \begin{bmatrix} \frac{-\Delta z_j}{2} \int_{-1}^0 A(\xi) d\xi + [(\rho e)_{j+1} - (\rho e)_j] \frac{\Delta z_j}{4} \int_{-1}^0 \xi A(\xi) d\xi \\ \frac{-\Delta z_j}{2} \int_0^1 A(\xi) d\xi + [(\rho e)_{j+1} - (\rho e)_j] \frac{\Delta z_j}{4} \int_0^1 \xi A(\xi) d\xi \end{bmatrix} \dots\dots\dots(25)$$

Performing the integration for planar geometry ( $A(\xi) = 1$ ) gives

$$\begin{bmatrix} \bar{E}_j \\ \bar{E}_{j+1} \end{bmatrix} = \frac{A\Delta z_j}{2} \begin{bmatrix} \frac{3}{4} & \frac{1}{4} \\ \frac{1}{4} & \frac{3}{4} \end{bmatrix} \begin{bmatrix} (\rho e)_j \\ (\rho e)_{j+1} \end{bmatrix} \dots\dots\dots(26)$$

The result is simply a weighted average of nodal values where the weighting factor matrix is geometry dependent. The time rate of change of energy content according to an implicit time integrator can be expressed as

$$\frac{d}{dt} \begin{bmatrix} \bar{E}_j \\ \bar{E}_{j+1} \end{bmatrix}^{n+1} = \left\{ \begin{bmatrix} \bar{E}_j \\ \bar{E}_{j+1} \end{bmatrix}^{n+1} - \begin{bmatrix} \bar{E}_j \\ \bar{E}_{j+1} \end{bmatrix}^n \right\} \frac{1}{\Delta t^{n+1}} \dots\dots\dots(27)$$

and linearizing in iteration space according to a Taylor series expansion gives

$$\frac{d}{dt} \begin{bmatrix} \bar{E}_j \\ \bar{E}_{j+1} \end{bmatrix}^{v+1} = \left\{ \begin{bmatrix} \bar{E}_j \\ \bar{E}_{j+1} \end{bmatrix}^v + \begin{bmatrix} \frac{\partial \bar{E}_j}{\partial s_j} & \frac{\partial \bar{E}_j}{\partial T_j} & \frac{\partial \bar{E}_j}{\partial T_{j+1}} \\ \frac{\partial \bar{E}_{j+1}}{\partial s_j} & \frac{\partial \bar{E}_{j+1}}{\partial T_j} & \frac{\partial \bar{E}_{j+1}}{\partial T_{j+1}} \end{bmatrix}^v \begin{bmatrix} \Delta s \\ \Delta T_j \\ \Delta T_{j+1} \end{bmatrix} \right\} - \begin{bmatrix} \bar{E}_j \\ \bar{E}_{j+1} \end{bmatrix}^v \left\{ \frac{1}{\Delta t^{v+1}} \dots\dots\dots(28)$$

where the sensitivity matrix entries are

$$\left. \begin{aligned} \frac{\partial \bar{E}_j}{\partial s_j} &= A \frac{\partial \Delta z_j}{\partial s} \left[ \frac{3}{8} (\rho e)_j + \frac{1}{8} (\rho e)_{j+1} \right] \\ \frac{\partial \bar{E}_{j+1}}{\partial s_j} &= A \frac{\partial \Delta z_j}{\partial s} \left[ \frac{1}{8} (\rho e)_j + \frac{3}{8} (\rho e)_{j+1} \right] \\ \frac{\partial \bar{E}_j}{\partial T_j} &= \frac{3A\Delta z_j}{8} (\rho C_v)_j \\ \frac{\partial \bar{E}_j}{\partial T_{j+1}} &= \frac{A\Delta z_j}{8} (\rho C_v)_{j+1} \\ \frac{\partial \bar{E}_{j+1}}{\partial T_j} &= \frac{A\Delta z_j}{8} (\rho C_v)_j \\ \frac{\partial \bar{E}_{j+1}}{\partial T_{j+1}} &= \frac{3A\Delta z_j}{8} (\rho C_v)_{j+1} \end{aligned} \right\} \dots\dots\dots(29)$$

The resulting linear system contributions for each jth element are

$$\begin{aligned}
 e(j) &= e(j) + \frac{1}{\Delta t^{n+1}} \frac{\partial \bar{E}_j}{\partial s_j} \\
 e(j+1) &= e(j+1) + \frac{1}{\Delta t^{n+1}} \frac{\partial \bar{E}_{j+1}}{\partial s_j} \\
 b(j) &= b(j) + \frac{1}{\Delta t^{n+1}} \frac{\partial \bar{E}_j}{\partial T_j} \\
 c(j) &= c(j) + \frac{1}{\Delta t^{n+1}} \frac{\partial \bar{E}_j}{\partial T_{j+1}} \\
 d(j) &= d(j) - \frac{1}{\Delta t^{n+1}} (\bar{E}_j^v - \bar{E}_j^n) \\
 a(j+1) &= a(j+1) + \frac{1}{\Delta t^{n+1}} \frac{\partial \bar{E}_{j+1}}{\partial T_j} \\
 b(j+1) &= b(j+1) + \frac{1}{\Delta t^{n+1}} \frac{\partial \bar{E}_{j+1}}{\partial T_{j+1}} \\
 d(j+1) &= d(j+1) - \frac{1}{\Delta t^{n+1}} (\bar{E}_{j+1}^v - \bar{E}_{j+1}^n)
 \end{aligned}
 \quad \dots (30)$$

The resulting linear system contributions for each jth element are

$$\begin{aligned}
 e(j) &= e(j) + \frac{\partial \dot{Q}_j}{\partial s} \\
 e(j+1) &= e(j+1) + \frac{\partial \dot{Q}_{j+1}}{\partial s} \\
 b(j) &= b(j) + \frac{\partial \dot{Q}_j}{\partial T_j} \\
 c(j) &= c(j) + \frac{\partial \dot{Q}_j}{\partial T_{j+1}} \\
 d(j) &= d(j) - \dot{Q}_j^v \\
 a(j+1) &= a(j+1) + \frac{\partial \dot{Q}_{j+1}}{\partial T_j} \\
 b(j+1) &= b(j+1) + \frac{\partial \dot{Q}_{j+1}}{\partial T_{j+1}} \\
 d(j+1) &= d(j+1) - \dot{Q}_{j+1}^v
 \end{aligned}
 \quad \dots (31)$$

### 3. RESULTS AND DISCUSSION

Assuming conduction and uniform heat flux distribution along the thickness will eliminate the convection and gas flux terms in the energy equation considering constant property, non-ablating, non-decomposing, one-dimensional, uniform density, planar slab with a specified constant heat

flux on the front face and an adiabatic back face. The governing equation, parameters associated with this problem are:

$$\int_{cs} \dot{q} \cdot dA + \frac{d}{dt} \int_{cv} \rho e dV = 0 \dots \dots (32)$$

**Table 2. Conduction problem parameters**

$T = 3500K$
$\dot{q} = 18.8MW/m^2$
$\rho = 1369 kg/m^3$
$k = 4 W/m^2K$
$C_v = 651.24 J/kg K$

The problem here is a linear convergence problem which undergoes iterative process to obtain the temperature distribution in the ablator.

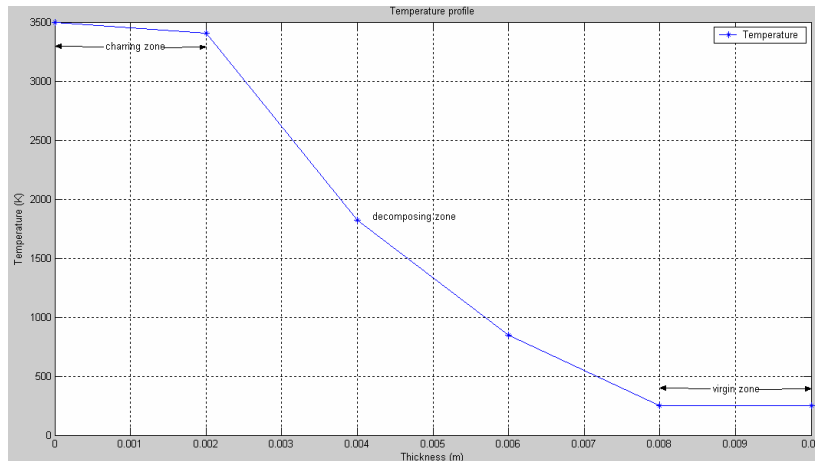


**Figure.3. Temperature profile**

#### 4. Conclusions

The method gives the acceptable temperature variation, showing less gradient in the charring zone and a step gradient in the decomposing zone where the density gradient does exist prompting the heat transfer towards the virgin zone but the constant temperature in the region protects the back-up structure from the heat transfer ensuring the safety of the system.

## 5. References

1. Blackwell, B. F., 1988 "Numerical Prediction of One-Dimensional Ablation Using a Finite Control Volume Procedure with Exponential Differencing," Numerical Heat Transfer, Vol. 14, No. 1, pp. 17-34.
2. Claud M.Pittman.,William D. Brewer "Analytical Determination of The effect of Thermal Property Variations on the performance of charring Ablator" Langley Research Center, Langley Station, Hampton, Va
3. Donald M. Curry, Dec 1965 "An Analysis of A Charring Ablation Thermal Protection System" Manned Spacecraft Center Huston Texas
4. Gerald Wayne Russell, "Analytic Modeling and Experimental Validation of Intumescent Behavior of Charring Heat-shield Materials" Propulsion and Structures Directorate Aviation and Missile Research, Development, and Engineering Center
5. J.L.Lin, C.S.Yang, Jun 2005 "Heat Transfer Analysis of Charring Ablators under Aerodynamic heating" Aircraft Engineering and Aerospace Technology, Volume: 77 Issue: 3 Page: 214 - 221
6. John D. Anderson.Jr, "Computational Fluid Dynamics" McGraw- Hill, Inc.
7. M Grujicic, C L Zhao, S B Biggers, J M Kennedy, and D R Morgan, Aug- 2005 "Heat transfer and effective thermal conductivity analyses in carbon-based foams for use in thermal protection systems"
8. Marvin B.Dow and Robert T, "Swann,"Determination of Effects of Oxidation on Performance of Charring Ablator"
9. Moyer, C. B., and Rindal, R. A., June 1968 "An Analysis of the Coupled Chemically Reacting Boundary Layer and Charring Ablator, Part II, Finite Difference Solution for the In-Depth Response of Charring Materials Considering Surface Chemical and Energy Balances," NASA CR-1061.
10. Rgale Wilson, "Thermo-physical Properties of Six Charring ablators from 140 to 700Kand Two Chars from 800 to 3000k" Langley Research Center, Langley Station, Hampton, Va
11. Robert T. Swann, "Approximate Analysis of the Performance of Char-Forming Ablator" Langley Research Center Langley Station, Hampton, Va.
12. Ronald K.Clark. "An Analysis of Charring ablator With Thermal Non-Equilibrium, Chemical kinetics and Mass transfer" Langley Research Center, Hampton, Va
13. V.Jones "Numerical Characterization and Computer Simulation of Heat Transfer in Solid Rocket Nozzles" PhD Thesis.
14. W.T.Engelke, C.M.Pyorn, Jr., C.D.Pears "Thermal and Mechanical Properties of a Non-degraded and Thermally Degraded Phenolic-carbon Composite". Southern Research Institute, Brimingham, Ala.

15. Xavier Bremond, Jean Pierre Humeau, Oct-1993 "Domain Identification Using a Landau Transform. Systems, Man and Cybernetics, apos; Systems Engineering in Service of Humans apos; Conference Proceedings, International Conference; vol-5, Issue 17-20, Page(s): 48-35.